A FRAMEWORK OF COLLABORATIVE CHANGE DETECTION WITH MULTIPLE OPERATORS AND MULTI-SOURCE REMOTE SENSING IMAGES

Xi Chen[1, 2] Jing Li[1, 2] Yunfei Zhang[1, 2] Liangliang Tao[1, 2] Wei Shen[3]*

[1] State Key Laboratory of Earth Surface Processes and Resource Ecology, Beijing Normal University, Beijing 100875, China; [2] Academy of Disaster Reduction and Emergency Management, Beijing Normal University, Beijing 100875, China; [3] College of Marine Sciences, Shanghai Ocean University, Shanghai 201306, China

ABSTRACT

This paper proposes a framework of change detection with multi-source remote sensing images through collaboration of multiple operators. Firstly, pre-processed images are distributed to different operators. Then the images are classified by the operators independently. Finally, with uploaded classification results, change detection result can be derived through evidential fusion based on PCR5 rule in the server. By making use of complementary and redundant information in the images, the framework can solve the problems of information loss, imprecision, inconformity or conflict in multi-source data. The framework is applied to detect a landslide barrier lake with multi-source images from Landsat7 and GF-1, results show that as the amount of operator and input image increases, the proposed framework performs better than commonly used major voting strategy for disaster mapping.

Index Terms— Change detection, multi-source image, evidential fusion, collaborative framework, remote sensing

1. INTRODUCTION

Change detection is widely used technique for land-cover monitoring. Many works devoting to change detection are based on single pair of pre- and post-change images (or bi-temporal change detection) [1]. However, with the limited two input images the results are not always reliable as many factors influence the result accuracy, such as the image quality, the calibration, registration, classification or manual interpretation accuracy, and so on. In order to overcome the shortcomings, multi-source images are usually employed for change detection. Moreover, classification or interpretation of the images are usually operated by different operators for efficiency, especially in emergency situations [2]. As a result, a framework for collaborative change detection with multi-source input data is in demand.

Change detection with multi-source data should face some problems such as information loss, data imprecision, data inconformity or even conflict. Data fusion strategies which have been successfully applied in fusing multi-source data, multi-temporal data, and different change indexes can

be a solution of these problems [3][4]. Firstly, through fusing complementary information from multi-source images, information loss resulting from cloud or shadow coverage, or image defects can be completed. Secondly, through fusing redundant information from multi-source data, imprecision and uncertainty can be reduced. Thirdly, with proper mechanisms to deal with data inconformity or conflict, robust change detection results can be derived after data fusion. Consequently, the data fusion strategies that introduced in the framework for collaborative change detection should be flexible and effective.

The mathematical theory of evidence that introduced by Dempster and Shafer (Dempster-Shafer evidence theory) can combine evidences with imprecision or uncertainty to obtain a final decision [5]. Evidential fusion method that developed from the theory appears to be a more flexible and general approach than the Bayesian one [6]. The method has been applied as a decision level image fusion method for both classification and change detection [3][4][6]. The researches mentioned above illustrate the potential of evidential fusion method for collaborative change detection. This paper aims at providing a change detection framework based on the Dempster-Shafer evidential fusion method for collaborative work with multiple operators and multi-source images.

2. METHODOLOGY

2.1. Image Pre-processing and Data Distribution

Before multi-source images distributed to operators, image pre-processing should be performed in the server. Image registration, radiometric and atmospheric calibration should be as accuracy as possible so that most of the interference factors from the images themselves can be eliminated. Subsequently, the pre-processed data can be randomly distributed to the operators, some auxiliary information such as brief description of the detected area and specifications of the images can be pushed to the operators, according to their experience about change detection.

2.2. Independent Image Classification

Image classification can be performed independently when the operators receive the distributed data. This process is the

only step that need large amount of human participation in the framework. Because as we know, most of the available algorithms for classification cannot perform better than an experienced operator. Ground truth ROIs that interpreted for supervised classification, or the classification results totally provided by manual interpretation should be uploaded for accuracy evaluation. Confusion matrixes of every classified image can be derived based on the ground truth data from the other operators as an objective result evaluation.

2.3. Change Detection Based on Evidential Fusion
In this framework, change detection can be performed based on evidential fusion method, after the server receives the classification results uploaded by different operators.

2.3.1. Evidence Construction
The change detection result from a pair of pre- and post-change classified image provides a change vector for each pixel. The vector is considered as evidence that can be measured for evidential fusion in the proposed framework.

Denoting Ψ the frame of discernment, which is a hypothesis set of land-cover change types. Elements of Ψ are single hypothesis denoted as $< \theta_x, \omega_y >$, which means the land- cover is classified as θ_x before change and become ω_y after change. Subsets of Ψ include the single hypothesis, the empty set $\varnothing$, the universal set Ψ, and unions of single hypothesis which are called compound hypotheses. We use a series values to measure the jth evidence E_j as follows:

$$E_j = [m_j(A_1), m_j(A_2), \cdots, m_j(A_k), m_j(\Psi)] \quad (1)$$

Where A_k represents the subset of Ψ, $m_j(\bullet)$ is the mass function of the jth evidence, and $m_j(A_k)$ is called a Basic Belief Assignment (BBA) of the evidence. There is no general way for modeling of the mass functions, but according to Dempster-Shafer evidence theory the values of BBA belongs to [0, 1] interval [5]. And there is:

$$m : \begin{cases} \sum_{A \subseteq \Psi} m(A) = 1 \\ m(\varnothing) = 0 \end{cases} \quad (2)$$

Denoting the confusion matrixes p_{t0} and p_{t1} correspond to pre- and post-change classified images T_{t0} and T_{t1}. In the proposed framework, definition of the BBAs for each pixel is based on its change vector and the confusion matrixes p_{t0} and p_{t1}. The elements of p_{t0} and p_{t1} should be converted to prediction positive rates as follows:

$$\begin{cases} P_{t0}(\theta_x, \theta_a) = \dfrac{p_{t0}(x,a)}{\sum_x p_{t0}(x,a)} \\ P_{t1}(\omega_y, \omega_b) = \dfrac{p_{t1}(y,b)}{\sum_y p_{t1}(y,b)} \end{cases} \quad (3)$$

Where $a, x = 0,1,2,\cdots, p$; $b, y = 0,1,2,\cdots, q$; p and q are the number of classes in classified images T_{t0} and T_{t1}. θ_0 and ω_0 are special classes that represent unknown class in

the images. $p_{t0}(x,a)$ and $p_{t1}(y,b)$ are elements in the confusion matrixes p_{t0} and p_{t1}, which represent the amount of pixels classified as class θ_x and ω_y while their ground true class are θ_a and ω_b, respectively. Assigning the belief value of a detected change vector (θ_x, ω_y) to all of the possible real change vectors $< \theta_a, \omega_b >$ as follows:

$$m(< \theta_a, \omega_b >) = P_{t0}(\theta_x, \theta_a) \cdot P_{t1}(\omega_y, \omega_b) \quad (4)$$

According to Dempster-Shafer's theory, the summation of the BBAs should satisfy equation (2). Denoting that:

$$M = \sum_a \sum_b m(< \theta_a, \omega_b >) \quad (5)$$

Then the BBAs can be normalized as follows:

$$m : \begin{cases} m(< \theta_a, \omega_b >) = P_{t0}(\theta_x, \theta_a) \cdot P_{t1}(\omega_y, \omega_b) / M \\ (a \neq 0, b \neq 0) \\ m(\Psi) = \sum_{a=0 \, or \, b=0} P_{t0}(\theta_x, \theta_a) \cdot P_{t1}(\omega_y, \omega_b) / M \\ m(\varnothing) = 0 \end{cases} \quad (6)$$

2.3.2. Evidential Fusion
The original evidential fusion rule provided by Dempster has some shortcomings in combining high conflicting information [7]. The Proportional Conflict Redistributions (PCR) rules are proved to be more suitable than Dempster's rule. In this paper, the PCR5 rule which developed from PCR rules are introduced to fuse the evidences as follows:

$$m_{PCR5}(C) = m_{12}(C) + \sum_{X_i \cap C = \varnothing} [\frac{m_1(C)^2 m_2(X_i)}{m_1(C) + m_2(X_i)} + \frac{m_2(C)^2 m_1(X_i)}{m_1(X_i) + m_2(C)}]$$
$$(m_1(C) + m_2(X_i) \neq 0, m_1(X_i) + m_2(C) \neq 0) \quad (7)$$

$$m_{12}(C) = \sum_{A_i \cap B_j = C} m_1(A_i) m_2(B_j) \quad (8)$$

Where, $A_i, B_j, X_i \subseteq \Psi$; $A_i \cap B_j = C$; $m_1(\bullet)$, $m_2(\bullet)$ come from two different evidences, $m_{12}(C)$ corresponds to the conjunctive consensus on C. If any denominator equals zero in (7) the fraction should be discarded. The evidential fusion rule can be applied iteratively. More evidences can be fused one after another as follows:

$$m = \{[(m_1 \oplus m_2) \oplus m_3] \oplus \cdots\} \oplus m_n \quad (9)$$

2.3.3. Decision Making
Decision making in the framework follows specific rule to decide which single hypothesis should be supported based on the BBAs of each pixel. The choice of this criterion remains application dependent. In this research, we follow the "maximum of belief" rule which indicates that the land-cover change type with the maximum belief function value is the final decision. The rule can be expressed as follows:

$$Bel(A_c) = \max_i \{Bel(A_i)\} \quad (10)$$

Where the belief function Bel is defined as:

$$Bel(A) = \sum_{B \subseteq A} m(B) \quad (\forall A \subseteq \Theta) \quad (11)$$

2.4. Global Process of the Framework

The global process of the framework is illustrated in Fig. 1 and described as follows:

Step 1: Data preparation and distribution. Collecting suitable data for change detection in the database, and then distributing the data to different operators after image pre-processing, together with necessary auxiliary information;

Step 2: Image classification. Different operators classify their images independently, and the classification results are evaluated by confusion matrixes based on the ground truth that uploaded by the other operators;

Step 3: Evidence construction. Selecting different pairs of pre- and post-change classified images with no repeat. Then, constructing the BBAs of evidence for each pixel following equations (3)-(6);

Step 4: Evidential fusion. Fusing BBAs of every evidence for each pixel following the PCR5 rule with equations (7)-(9), then the fused BBAs of each pixel can be derived;

Step 5: Decision making. Detecting the land-cover change type for all pixels following the "maximum of belief" rule with equations (9)-(11). Then, the final change detection map can be derived.

3. APPLICATION

3.1. Data and Study Area

An Ms 6.5 earthquake took place in Ludian county, China, on 3 August, 2014, and triggered a landslide barrier lake that flooded villages near the Niulan River and threatened the safety of both upstream and downstream residents (103.379°~103.446°E, 26.997°~27.042°N).

The proposed method is applied to detect the barrier lake based on 6 multi-source images come from the ETM+ SLC off sensor on Landsat7, PMS2 sensor, WFV1 sensor and WFV3 sensor on the Chinese satellite GF-1, respectively. Affected by weather conditions, all images are partially covered by thick clouds and the ETM+ SLC off images are with stripes. The images are tagged according to their acquisition date (see in Fig. 2), the 3 images acquired before disaster are tagged as (1), (2), (3), the other images acquired after disaster are tagged as (1*), (2*), (3*). Auxiliary information of the input images is listed in Table. 1.

3.2. Data Processing and Results

Each input image was classified into 3 main classes by the Maximum Likelihood Classification (MLC) algorithm. The 3 classes were: (1) Water (include rivers and watercourse); (2) Land (include vegetation, bared land and built-up land); (3) Unknown (include clouds and shadows). The samples for training and calculating the confusing matrixes were independently extracted by visual interpretation, and the classification accuracy is various in different images (as listed in Table2). With 3 pre-disaster images and 3 post-disaster images, at most 9 different pairs of images can be produced for evidence construction.
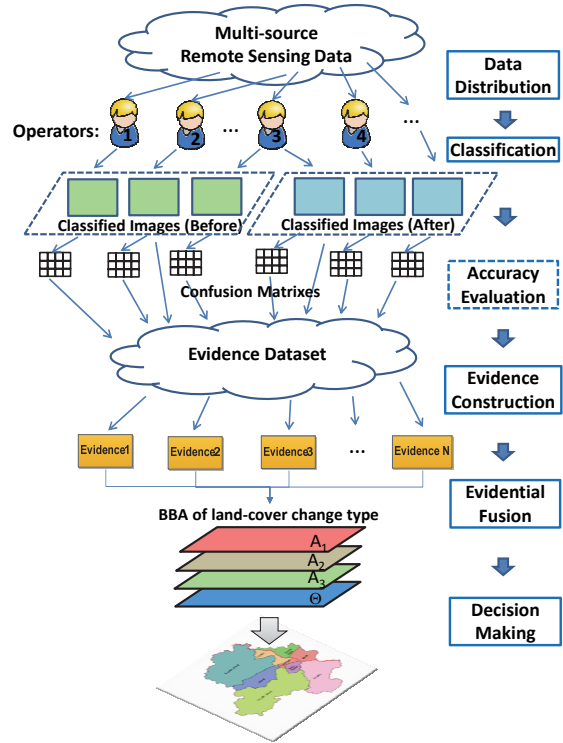
Fig. 1 Framework of the proposed method for collaborative change detection.

Specification	Parameter					
Data Tag	(1)	(2)	(3)	(1*)	(2*)	(3*)
Acquisition Date	06-25	07-04	07-23	08-05	09-11	10-08
Satellite	GF-1	Landsat7	GF-1	GF-1	GF-1	Landsat7
Sensor	PMS2	ETM+	WFV1	PMS2	WFV3	ETM+
Resolution(m)	8	30	16	8	16	30
Number of band	4	7	4	4	4	7
Image Defect	Cloud (11.5%)	Cloud +Stripe (28.2%)	Cloud (7.1%)	Cloud (32.8%)	Cloud (7.7%)	Cloud +Stripe (18.3%)

Table 1. Basic specifications of the input data.

We calculated the change detection results with different amount of evidences (from 2 to 9 evidences) and evaluated the average accuracy of the results by the overall accuracy and Kappa coefficient. Furthermore, the proposed method was compared with the majority voting strategy which is commonly used for data fusion that the land-cover change type is identified according to the majority of the operators. The result evaluation indexes are listed in Table 3. The average Kappa increases from 0.58 to around 0.80 as the number of evidences increases from 2 to 9. With more than 6 evidences to be fused, the proposed method performs better than the majority voting strategy, especially on the Kappa index. After fusing all of the available evidences, the change detection results provided by the proposed method and majority voting method, as well as the ground truth derived from manual interpretation are shown in Fig.2.

Image tag	User accuracy (%)			Overall accuracy (%)	Kappa coefficient
	Water	Land	Unknown		
(1)	89.52	95.54	98.10	94.49	0.92
(2)	96.52	95.74	99.60	97.48	0.96
(3)	96.10	88.84	93.43	92.02	0.88
(1*)	99.73	97.84	99.14	98.74	0.98
(2*)	98.87	98.78	99.40	98.99	0.98
(3*)	58.35	53.42	82.63	59.13	0.38

Table 2. Classification accuracy of the images classified by the MLC algorithm.

Amount of evidences	Proposed Method		Majority Votin	
	Overall accuracy(%)	Kappa coefficient	Overall accuracy(%)	Kappa coefficient
1	-	-	98.07	**0.6071**
2	96.31	0.5819	**98.26**	**0.6381**
3	98.28	0.7228	**98.64**	**0.7433**
4	98.21	**0.7292**	**98.55**	0.7151
5	98.29	0.7266	**98.71**	**0.7583**
6	**98.73**	**0.7777**	98.72	0.7535
7	**98.83**	**0.7799**	98.72	0.7772
8	**98.85**	**0.7988**	98.82	0.7884
9	**98.87**	**0.7968**	98.85	0.7761

Table 3. Average overall accuracy and kappa coefficient of the change detection results with different amount of evidences.
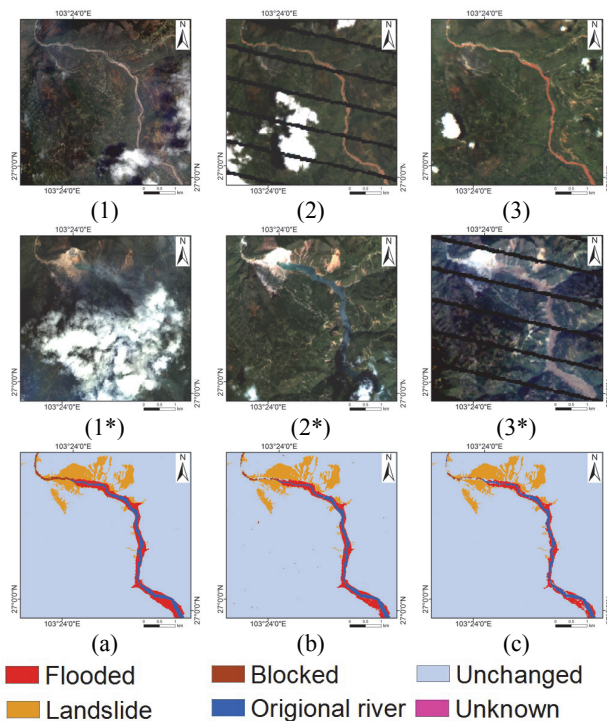
Fig. 2 The input images and the change detection results. (1), (2), (3) and (1*), (2*), (3*) are input images as tagged in Table. 1; (a) the ground truth by manual interpretation; (b) the change detection result by Dempster-Shafer Fusion; (c) the change detection result by Majority Voting (The original river (blue) and landslide area (yellow) are added manually to indicate relative position).

3.3. Conclusion

With multi-source remote sensing images and multiple operators employed for change detection, a collaboration framework is in demand. The Dempster-Shafer evidence theory and the PCR5 rule is introduced to achieve that goal. The proposed framework distributes multi-source images to different operators for classification and derives the change detection result by fusing the classified images uploaded by various operators. Benefiting from the Dempster-Shafer evidence theory, the framework is still feasible even though there are information loss, imprecision, inconformity or conflict problems in the input data. Application shows that clouds and stripes in the input images do not prevent the framework to generate a cloud-free change detection map. What's more, as the number of input image increases, the proposed framework will perform better than major voting strategy. This paper indicates the effectiveness and flexibility of the proposed framework for change detection.

4. ACKNOWLEDGEMENT

5. REFERENCES

[1] P. Coppin, I. Jonckheere, K. Nackaerts, et al., "Digital change detection methods in ecosystem monitoring: a review". *Int. J. Remote Sens.*, 25(9), pp. 1565-1596, 2004.

[2] M. Xu, C. Cao, H. Zhang, et al., "Change detection of the tangjiashan barrier lake based on multi-source remote sensing data". In *Proc. Int. Geosci. Remote Sens. Symp. (IGARSS)*, Cape Town, South Africa, vol. 1, pp. 2683-2686, 2009.

[3] P. Du, S. Liu, J. Xia, et al., "Information fusion techniques for change detection from multi-temporal remote sensing images". *Information Fusion*, 14(1), pp. 19-27, 2013.

[4] Z. Liu, G. Mercier, J. Dezert, et al., "Change detection in heterogeneous remote sensing images based on multidimensional evidential reasoning". *IEEE Geosci. Remote Sens. Lett.*, 11(1), pp. 168-172, 2014.

[5] G. Shafer, *A Mathematical Theory of Evidence*. Princeton, NJ: Princeton University press, 1976.

[6] S. Lehegaratmascle, I. Bloch, D. Vidalmadjar, "Application of Dempster-Shafer evidence theory to unsupervised classification in multisource remote sensing". *IEEE Trans. Geosci. Remote Sens.*, 35(4), pp. 1018-1031, 1997.

[7] F. Smarandache and J. Dezert, "Information fusion based on new proportional conflict redistribution rules," in *Proc. of 8th Int. Conf. on Information Fusion*, USA, 2005.